Comparative Study of Feeding Techniques for Three-Dimensional Cavity Resonators at 60 GHz

Jong-Hoon Lee, *Student Member, IEEE*, Stéphane Pinel, *Member, IEEE*, John Papapolymerou, *Senior Member, IEEE*, Joy Laskar, *Fellow, IEEE*, and Manos M. Tentzeris, *Senior Member, IEEE*

***Abstract*—In this paper, various topologies of feeding structures are comparatively evaluated for 60-GHz three-dimensional integrated cavity resonators used in three-dimensional integrated RF modules. Three excitation techniques (slot excitation with a shorting via, slot excitation with a $\lambda g/4$ open stub, probe excitation) have been evaluated using simulated and measured data. The probe excitation is demonstrated as an attractive option for wideband applications due to its relatively wide bandwidth performance ($\sim$1.8%) and the strongest external coupling. The slot excitation with an open stub outperforms the other techniques, exhibiting the lowest insertion loss ($\sim$0.84 dB) for a 3-dB bandwidth of about 1.5% centered at 59.2 GHz and has the simplest fabrication.**

***Index Terms*—Cavity resonators, low-temperature cofired ceramic (LTCC), millimeter-wave (mmW), probe excitation, slot excitation, system-on-package (SOP), 3-D integration, unloaded quality factor (Qu).**

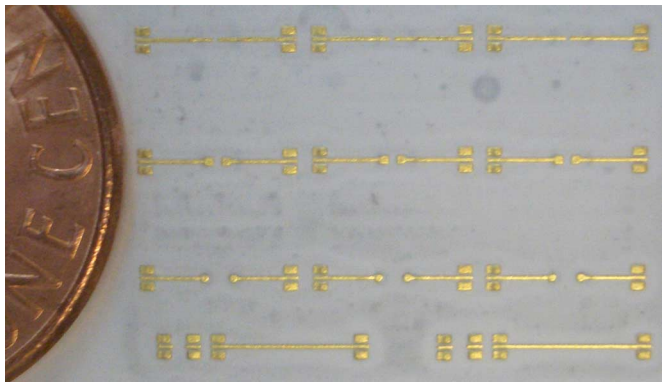

Fig. 1. Top view of fabricated Circuits in low-temperature cofired ceramic (LTCC). LTCC cavity resonators with three different excitation techniques are fabricated. (first row: three samples with open stubs, second row: three samples with shorting vias, third row: three samples with probe excitation, fourth row: two samples of open pads and thru lines).

I. Introduction

RECENTLY, the multilayer system-on-package (SOP) approach has emerged as an effective solution for the easy 3-D integration of embedded functions since it is based on multilayer technology using low-cost and high-performance materials. It aims to replace many discrete and surface-mounted components by embedded components [1]. As the demand for high-density, low manufacturing cost and high-performance RF and millimeter-wave (mmW) wireless systems increases, low-temperature cofired ceramic (LTCC) has been widely used as a packaging material in RF and mmW applications because of its mature multilayer fabrication capability, stability, and relatively low cost [2]. Using LTCC multilayer technologies, integrated waveguides (IWGs) and cavity filters can be easily realized in compact configurations by vertically stacking them on top of each other.

The IWG and cavities [3]–[8] employing metallic via arrays as sidewalls have been commonly utilized to design microwave and mmW components such as oscillators [4], power dividers [5] and, filters [6], [7] because of their high quality factor (Q), high power capacity, and great potential of 3-D integration compared to the planar circuits. Many previous publications [8]–[12] on low-loss and compact filters in LTCC technology have experimentally verified its advantages for passive circuits such as cavity resonators.

The type of the feeding structure is of great significance in the design of the cavity resonators, especially in the mmW frequencies, because it can significantly alter the circuit performance (insertion loss, unloaded Q ($Q_{\rm u}$), accurate resonant frequency). The microstrip line feeding through a coupling slot in the ground plane was proposed by Pozar [13] and has been applied to various mmW patch antennas [13], [14] and cavity resonators/filters [7], [15]. The 3-D duroid-based electromagnetic band-gap (EBG) cavity resonators/filters presented in [7] have demonstrated their compatibility with current printed circuit board (PCB) fabrication technology and the reconfigurability through the use of electronically switched post elements. Ito *et al.* [16] developed 60-GHz (V-band) alumina waveguide filters using the coplanar waveguide (CPW) I/O ports. It exhibited less than 3-dB insertion loss and a good stop-band rejection near the pass-band. To achieve high-Q ($>$1000), a microstrip-connected probe has been weakly coupled to a cavity resonator at Ka band [8]. Although various cavity excitation techniques have been investigated by several authors [8], [17] over the past, it is still challenging to choose the best technique especially for mmW applications because of their different operating characteristics and tradeoffs based on the demands considered.

This paper presents for the first time an experimental evaluation of 60 GHz 3-D LTCC cavity resonators fed by three different excitation techniques as shown in Fig. 1 (1) slot excitation with a shorting via, 2) slot excitation with a $\lambda_{\rm g}/4$ open stub,

Manuscript received July 22, 2005; revised February 16, 2006 and July 25, 2006. This work was supported in part by the National Science Foundation (NSF) under CAREER Award ECS-9984761 and Grant ECS-0313951, in part by the Georgia Electronic Design Center, and in part by the Georgia Institute of Technology Packaging Research Center.

The authors are with the School of Electrical and Computer Engineering, Georgia Institute of Technology, Atlanta, GA 30332 USA (e-mail: jonglee@ece.gatech.edu).

Color versions of one or more of the figures in this paper are available online at http://ieeexplore.ieee.org.

Digital Object Identifier 10.1109/TADVP.2006.890205

and 3) probe excitation). The performance of the three excitation schemes is comparatively evaluated in terms of S-parameters, bandwidth, external coupling ($Q_{\rm ext}$), $Q_{\rm u}$, and fabrication accuracy/simplicity based on electromagnetic simulations and experimental results. Details of the design procedure of each technique are discussed.

II. Design of Cavity Resonator

The design of the presented multilayer LTCC cavity resonator is based on the conventional rectangular cavity resonator approach [7]. The 60-GHz resonant frequency of $TE_{\rm mnl}$ mode is given by [18]

$$f_{\rm res} = \frac{c}{2\pi\sqrt{\varepsilon_r}}\sqrt{\left(\frac{m\pi}{L}\right)^2 + \left(\frac{n\pi}{H}\right)^2 + \left(\frac{l\pi}{W}\right)^2} \quad (1)$$

where $f_{\rm res}$ is the resonant frequency, c the speed of light in vacuum, $\varepsilon_{\rm r}$ the dielectric constant of the cavity filling, L the length of cavity, W the width of cavity, and H the height of cavity. The initial dimensions of the cavity with perfect electric conductor (PEC) walls can be determined using (1) for TE_{101} mode by simply indexing $m = 1$, $n = 0$, and $l = 1$. A height (H) of 0.3 mm was determined to satisfy both the compactness requirement and a relatively high Q value (>350). Then, the vertical PEC walls can be replaced by via fences to eliminate the surface currents. The final dimensions of the cavity are optimized using the HFSS simulator. Since the feeding structure affects not only the physical dimensions but also the electromagnetic behavior of the cavity, it is a key issue to choose the optimal type of feeding structure in order to achieve low insertion loss, high $Q_{\rm u}$, and accurate resonant frequency.

To minimize the field leakage, the spacing between the via posts in the sidewalls has to be less than half guided wavelength ($\lambda_{\rm g}/2$) at the highest frequency of interest [7]. Also, it has been experimentally proven that the double rows of vias are sufficient to suppress the field leakage and enhance Q [7]. In the full-wave simulations, double and triple rows exhibit almost the same characteristics such as an insertion loss of 1.14 dB, while a single row exhibits 1-dB higher insertion loss due to a higher leakage. However, the triple rows of vias have been implemented in fabrication to ensure a high level of leakage block that may have been compromised due to the simulation error and the fabrication accuracy. In this paper, the minimum via pitch and the minimum via diameter have been set to 390 and 130 μm, respectively.

The $Q_{\rm u}$ of a rectangular cavity resonator can be obtained by the following equation: [19]

$$Q_u = \left(\frac{1}{Q_{\rm cond}} + \frac{1}{Q_{\rm dielec}}\right)^{-1} \quad (2)$$

where $Q_{\rm cond}$ is related to the lossy conducting walls, and $Q_{\rm dielec}$ to the dielectric losses. The quality factors $Q_{\rm cond}$ and $Q_{\rm dielec}$ can be calculated, respectively, using [19]

$$Q_{\rm cond} = \frac{(kWL)^3 H\eta}{2\pi^2 R_m(2W^3H + 2L^3H + W^3L + L^3W)} \quad (3)$$

$$Q_{\rm dielec} = \frac{1}{\tan(\delta)} \quad (4)$$

where k is the wave number, R_m is the surface resistance of the cavity ground planes, η is the wave impedance of the LTCC filled resonator, L, W, and H are, respectively, the length, width, and height of the cavity resonator, and $\tan(\delta)$ is the loss tangent of the LTCC substrate filling the cavity resonators. The quality factor (2)–(4) of a rectangular cavity can be used in the cavity using via-array sidewalls due to effective performance of the via-arrays, which almost matches the performance of the PECs [7], [8].

The loaded quality factor ($Q_{\rm l}$) can be obtained by adding the losses ($Q_{\rm ext}$) of the external excitation circuit to the $Q_{\rm u}$ as expressed in [19]

$$Q_l = \left(\frac{1}{Q_u} + \frac{1}{Q_{\rm ext}}\right)^{-1} \quad (5)$$

The theoretical Q values can be extracted from the simulated performances of a weakly coupled cavity resonator using the following equations [19]:

$$Q_l = \frac{f_{\rm res}}{\Delta f} \quad (6)$$

$$S_{21}({\rm dB}) = 20\log_{10}\left(\frac{Q_l}{Q_{\rm ext}}\right) \quad (7)$$

$$Q_u = \left(\frac{1}{Q_l} - \frac{1}{Q_{\rm ext}}\right)^{-1} \quad (8)$$

where Δf is the 3-dB bandwidth.

The weak external coupling (S21∼20 dB) is imperative verifying the $Q_{\rm u}$ of the cavity resonator. The comparison between the theoretical and the HFSS-based $Q_{\rm u}$ values is discussed in Section III. The external coupling strength of three feeding techniques is also compared in Section III based on the $Q_{\rm ext}$ measured from strongly coupled resonators using (6) and (7). All fabricated resonators were measured using the Agilent 8510C Network Analyzer and Cascade Microtech probe station with 250-μm-pitch air coplanar probes. A standard short-open-load-thru (SOLT) method was employed for calibration.

III. Comparison of Excitation Techniques

A. Slot Excitation With a Shorting Via

Fig. 2 shows (a) the top view, (b) a 3-D overview, and (c) the side view of the proposed structure. Microstrip lines are utilized to excite the resonator through coupling slots etched in the top metal layer (metal 2) of the cavity as shown in Fig. 2(c). In order to maximize the magnetic coupling by maximizing magnetic currents, the microstrip lines are terminated with a physical short circuit realized by a metallic via. The spacing [VE in Fig. 2(a)] between the center of the via and the edge of the slot is determined to be 165 μm according to the LTCC design rules we used.

The accurate design of the external coupling slots is a key issue to achieve a high-Q cavity resonator. The external coupling factor is directly related to the input resistance and reactance that can be controlled by the position and size of the coupling aperture [20]. To determine the dimensions of the slots for the optimum response, the coupling slots are initially located at a quarter of the cavity length [SP in Fig. 2(a)] from the edge of the cavity to maximize the coupling [7], and then the slot width [SW in Fig. 2(a)] is varied with the constant slot length [SL $\approx \lambda{\rm g}/4$

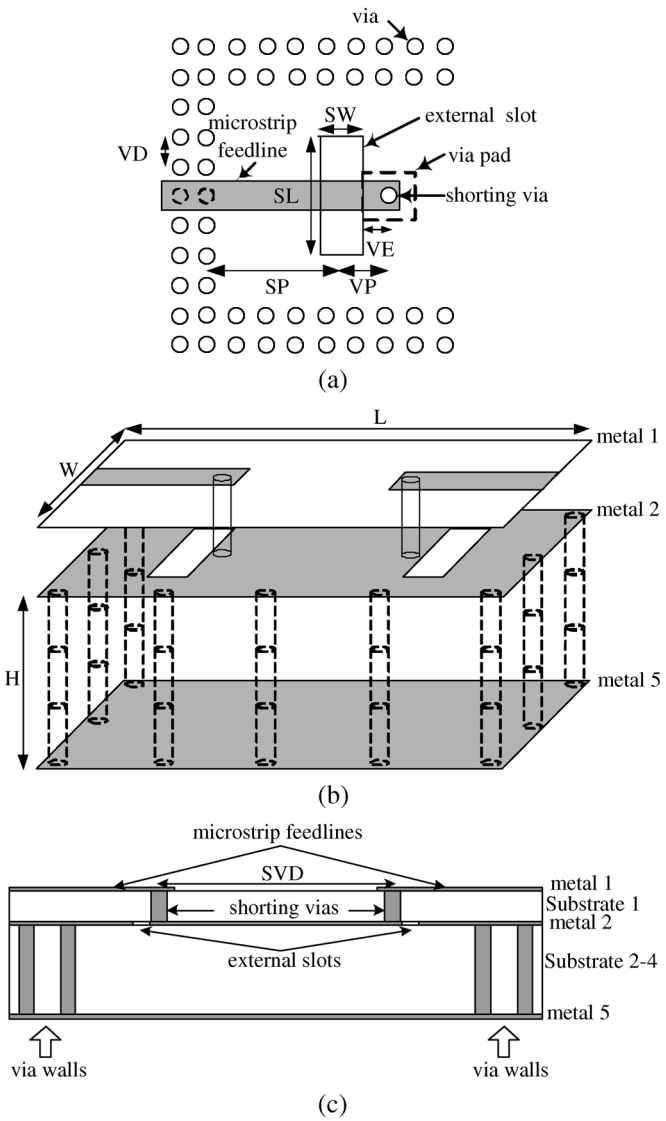

Fig. 2. LTCC cavity resonator employing slot excitation with a shorting via. (a) Top view of feeding structures. (b) 3-D overview. (c) Side view of the proposed resonator.

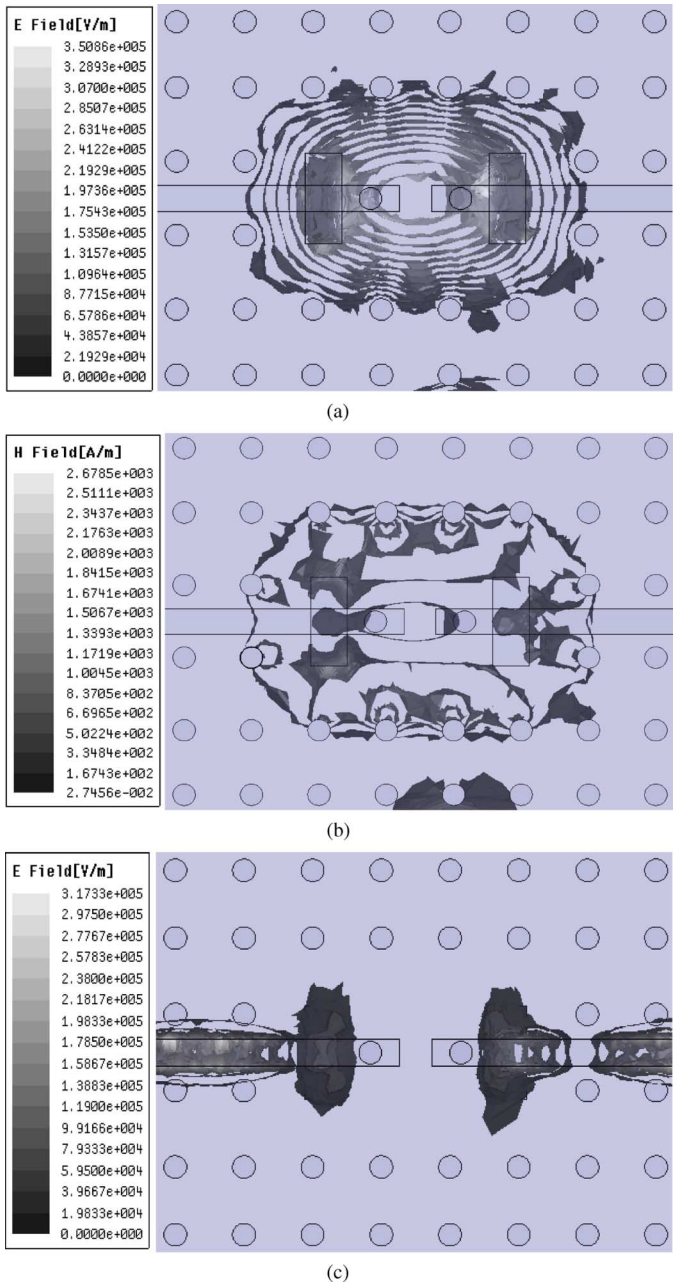

Fig. 3. (a) Electric field distribution and (b) magnetic field distribution inside the cavity [substrate 2–4 in Fig. 2(c)] using shorting vias at resonant frequency (= 59.4 GHz) (c) electric field distribution of the top substrate layer [substrate 1 in Fig. 2(c)].

at 60 GHz in Fig. 2(a)]. As the slot width increases, the radius of the simulated impedance locus increases, which denotes a strong external coupling. The dimensions of the coupling slots have been determined to be 0.538×0.21 mm^2 ($\approx 0.21\lambda_g \times 0.08\lambda_g$). Then, the position of the slots is adjusted to obtain the desired insertion loss, resonant frequency, and input impedances. The optimized results for resonant frequency (59.9 GHz), insertion loss (1.07 dB), and bandwidth (1.5%) are obtained with SP $= 0.4475$ mm $(\approx 0.19\lambda_g)$ [Fig. 2(a)].

Fig. 3 shows (a) the electric field distributions, (b) the magnetic field distributions inside the cavity surrounded by rows of vias, and (b) of the top substrate. It is clearly observed that two rows of vias are sufficient to block the field leakage through vias in Fig. 3(a). Nevertheless, in the fabrication, three rows of via posts were used to ensure a high level of leakage block with respect to both the simulation error and the fabrication accuracy as mentioned in Section II. The simulation of the top substrate [Fig. 3(c)] shows the decoupling between the two microstrip feedlines because of shorted vias providing the necessary shielding. All final design parameters are summarized in Table I.

The proposed cavity resonator was fabricated in LTCC multilayer substrate ($\varepsilon_r = 5.4, \tan\delta = 0.0015$). The dielectric thickness per layer is 100 μm, and the metal thickness is 9 μm. Its photograph is shown in Fig. 4. The overall size was 3.8 mm $\times$ 3.2 mm $\times$ 0.3 mm (including the CPW measurement pads).

The measured insertion and reflection loss of the fabricated cavity are compared with the simulated results in Fig. 5. The measured insertion loss is 1.28 dB, which is 0.21 dB higher than

TABLE I
DESIGN PARAMETERS OF CAVITY RESONATORS USING THREE DIFFERENT EXCITATION TECHNIQUES

Cavity Resonator using Shorting Vias		**Cavity Resonators using Open Stubs**		**Cavity Resonators using Probes**	
Design Parameters	*Dimensions (mm)*	*Design Parameters*	*Dimensions (mm)*	*Design Parameters*	*Dimensions (mm)*
effective cavity length (L)	1.95	effective cavity length (L)	1.95	effective cavity length (L)	1.95
effective cavity width (W)	1.318	effective cavity width (W)	1.318	effective cavity width (W)	1.276
effective cavity height (H)	0.3	effective cavity height (H)	0.3	effective cavity height (H)	0.3
slot positioning (SP)	0.4475	slot positioning (SP)	0.4475	probe positioning (PP)	0.4475
shorted via positioning (VP)	0.7175	open stub length (OSL)	0.485	via pad radius (rad1)	0.165
slot length (SL)	0.538	slot length (SL)	0.538	aperture radius (rad2)	0.24
slot width (SW)	0.21	slot width (SW)	0.21		
via pitch (VD)	0.39	via pitch (VD)	0.39	Via pitch (VD)	0.39
via diameter	0.13	via diameter	0.13	via diameter	0.13
via rows	3	via rows	3	via rows	3

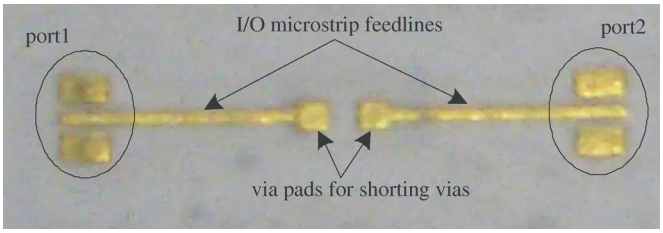

Fig. 4. Photograph of the fabricated cavity resonator using slot excitation with a shorting via.

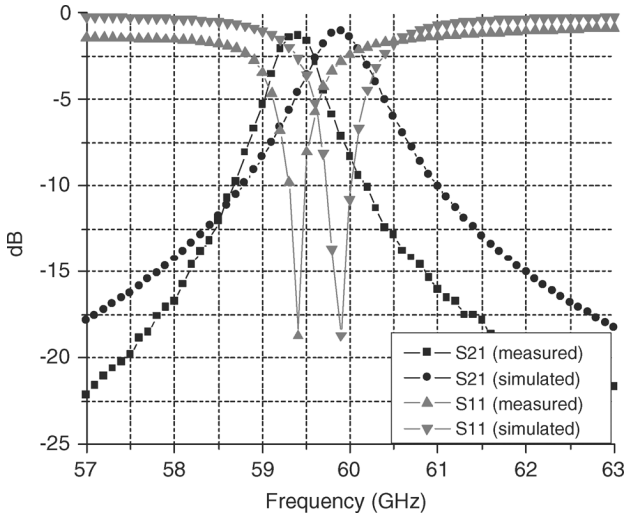

Fig. 5. Comparison between measured and simulated S-parameters (S11 and S21) of a cavity resonator using slot excitation with a shorting via.

the simulated value, while return losses match closely. The main source of this discrepancy might be the radiation loss from the feeding line. The center frequency shift from 59.9 to 59.4 GHz can be attributed to the fabrication accuracy (dielectric constant variation, slot positioning affected by the alignment between layers, via positioning tolerance, shrinkage, and layer thickness tolerance). Also, the resonator exhibits a 3-dB bandwidth of about 1.18% at the center frequency of 59.4 GHz, compared to 1.5% from the simulated model. The narrow bandwidth in measurements might be due to the fabrication accuracy of the slot design that has been optimized for the original resonant frequency and not for the shifted frequency. Also, in the calibration task, the calibration kit containing information about the Cascade probes and Cascade impedance standard substrates (ISS) was loaded into SOLT dialog box supported by "Wincal" software. Wincal gives us the ability to de-embed capacitance effects of CPW open pads and inductive effects of short pads from device measurements, but it cannot effectively remove all parasitic effects at this high-frequency range so that we can expect the band-limiting effect to S21 performance as well. The extracted $Q_{\rm u}$ from the weakly coupled resonators in full-wave simulations was found to be 360 that is lower than the theoretical $Q_{\rm u}$ of 372 obtained using (2)–(4). The $Q_{\rm ext}$ was measured to be 73.23.

B. Slot Excitation Using a $\lambda_{\rm g}/4$ Open Stub

Fig. 6 shows (a) the top view of the feeding structure and (b) the side view of the microstrip-fed cavity resonator using a $\lambda_{\rm g}/4$ open stub slot excitation technique. The structure is the same as in the previous Section III-A, except that the microstrip feed-line is terminated with a $\lambda_{\rm g}/4$ open stub beyond the slot.

All design parameters are summarized in Table I. The magnitude of the electric field distribution inside the cavity is simulated at the resonant frequency of 59.8 GHz and its efficient containment is clearly observed in Fig. 7(a). However, the extended stubs generate electrical coupling effects between the feed-lines and the substrate as shown in Fig. 7(b). The photograph of the LTCC is shown in Fig. 8.

Fig. 9 shows the simulated and the measured S-parameters of the cavity resonator with open stubs. Good correlation is observed for insertion loss. The resonator measurements exhibit

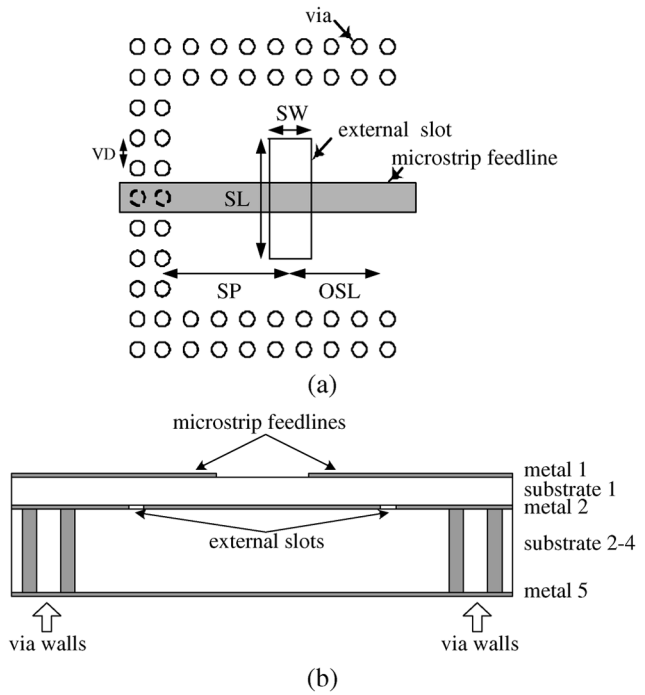

Fig. 6. LTCC cavity resonator employing slot excitation with an open stub. (a) Top view of feeding structure. (b) Side view of the proposed resonator.

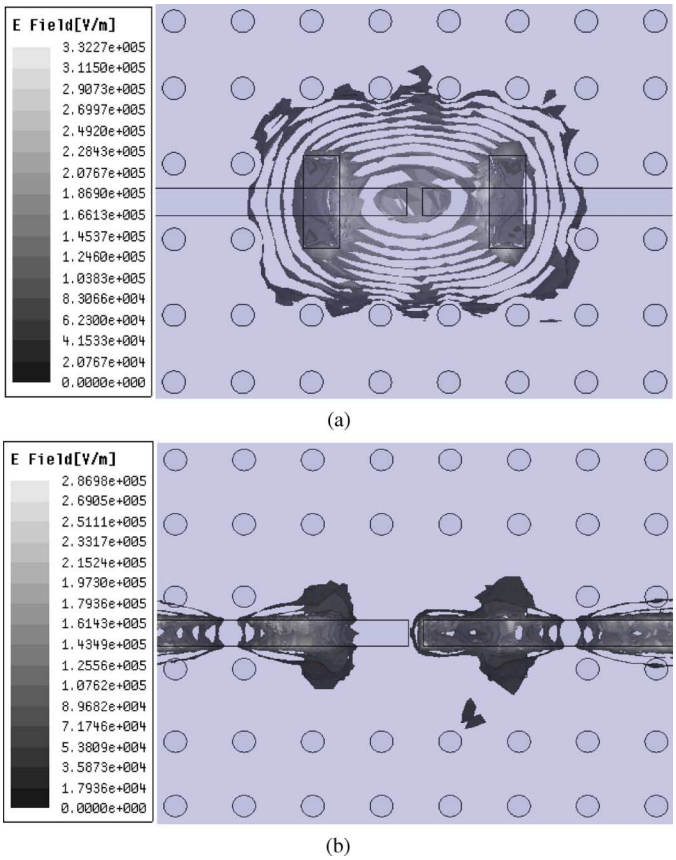

Fig. 7. (a) Electric field distribution inside the cavity using slot excitation with an open stub at resonant frequency (= 59.2 GHz). (b) Electric field distribution of the top substrate layer [substrate 1 in Fig. 6(b)].

an insertion loss <0.84 dB, a return loss about 20.59 dB at the center frequency of 59.2 GHz, and a 3-dB bandwidth about

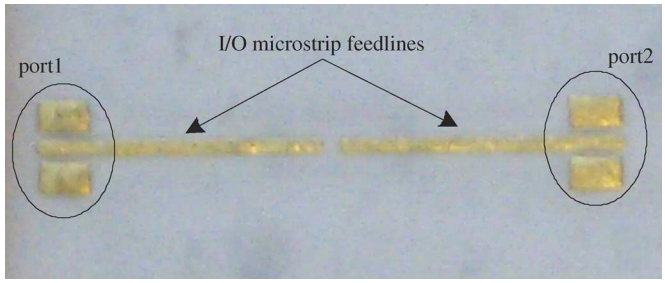

Fig. 8. Photograph of the fabricated cavity resonator using slot excitation with an open stub.

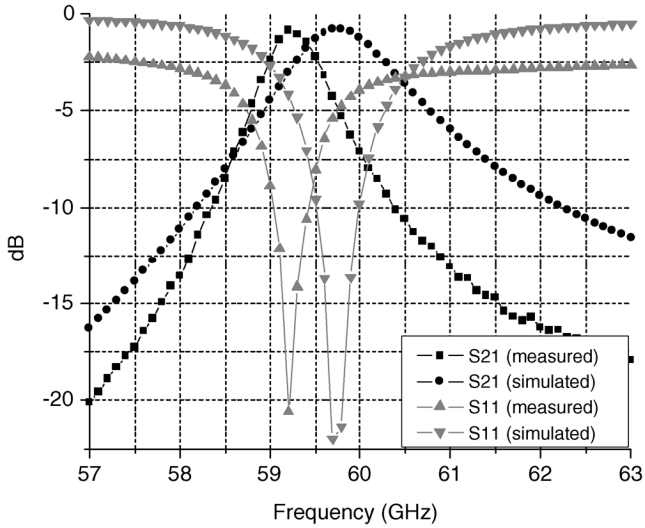

Fig. 9. Comparison between measured and simulated S-parameters (S11 and S21) of a cavity resonator using slot excitation with an open stub.

1.5% at the center frequency. The simulation shows almost the same insertion loss and return loss but an increased bandwidth of 2.3% around the center frequency of 59.8 GHz. The narrow bandwidth in measurements might be due to the fabrication accuracy of the slot design that has been optimized for the original resonant frequencies and not for the shifted frequencies. The frequency downshift between measurements and simulations is similar to the one observed in Section III-A. The long I/O feed lines that are terminated with 0.085-mm gap between them could be responsible for the asymmetrical response due to the parasitic cross-coupling and substrate coupling effects as shown in Fig. 7(b). The excitation technique using a shorting via takes advantage of the significantly reduced coupling between the two microstrip feed-lines because of the vias providing the necessary shielding. Using (6)–(8), the simulated $Q_{\rm u}$ was found to be 367, which is approximately 2% higher than that with a shorting via. The measured $Q_{\rm ext}$ was 60.52 which is lower than a shorting via ($Q_{\rm ext} \sim 73.23$).

C. Probe Excitation

Fig. 10 illustrates (a) the top view of the feeding structure and (b) the side view of via-fed cavity resonator. The probe length [PL in Fig. 10(b)] and the probe position [PP in Fig. 10(a)] are the dominant design factors to achieve the maximum coupling from the probe to the cavity and are investigated with the aid

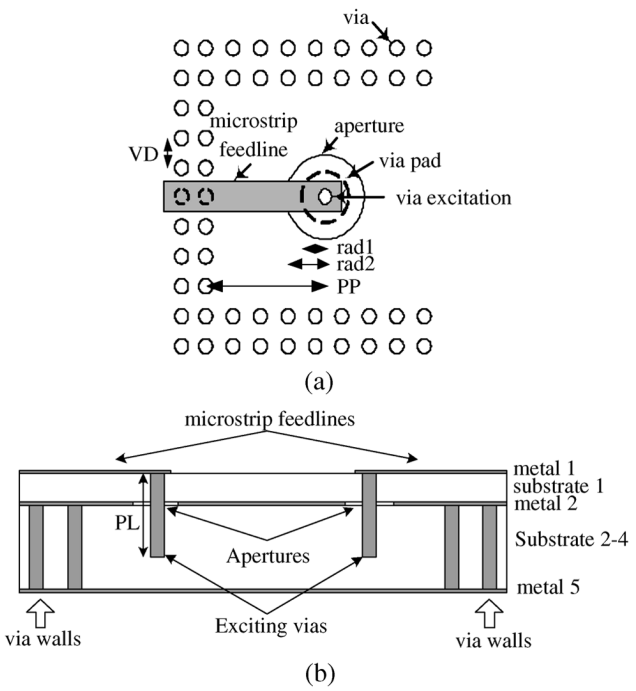

Fig. 10. LTCC cavity resonator employing probe excitation. (a) Top view of feeding structure. (b) Side view of the proposed resonator.

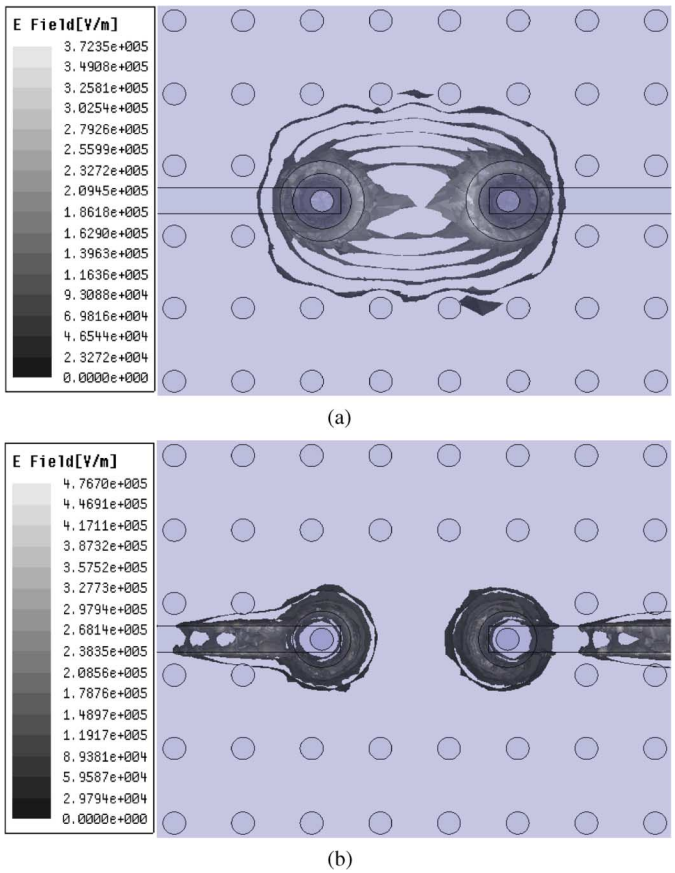

Fig. 11. (a) Electric field distribution inside the cavity using probe excitation at resonant frequency ($= 59.8$ GHz). (b) Electric field distribution of the top substrate layer [substrate 1 in Fig. 10(b)].

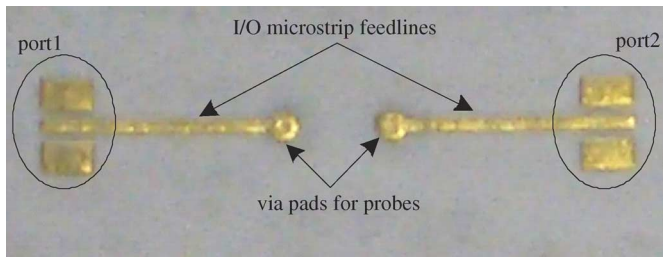

Fig. 12. Photograph of the fabricated cavity resonator using probe excitation.

of HFSS. For maximum coupling with the TE_{101} mode in the cavity, the probe [exciting vias in Fig. 10(b)] descends into the cavity through a circular aperture [aperture in Fig. 10(a)] etched in the second metal layer [metal 2 in Fig. 10(b)] up to the location of the maximum electric field at a distance of half of the cavity height. In our design, the excitation probe consists of three vias vertically stacked and penetrates three substrate layers [substrate 1–3 in Fig. 10(b)]. The size of the via pads is kept to the minimum size allowed by the LTCC design rules to minimize the parasitic effects.

The effect of the probe position was investigated in terms of insertion loss, bandwidth, and input impedance. The probes were initially located at the edge of the cavity, and then moved toward the center to achieve the strongest coupling possible. The probe position [PP in Fig. 1(0a)] has been found to be optimum at the same location $(\mathrm{PP} = 0.4475\ \mathrm{mm})$ as the slot position in Sections III-A and III-B. The effect of the aperture size was also investigated. It was observed from the simulations that the bandwidth gets wider and the insertion loss lower with the decrease of the aperture radius [rad2 in Fig. 10(a)].

The dimension of the cavity composed of the via walls was determined to be $1.95 \times 1.276\ \mathrm{mm}^2$ $(\approx 0.77\lambda_g \times 0.5\lambda_g)$. The width of this cavity is 42 μm smaller than the ones in Sections III-A and III-B. The resonant frequency shifts down because of the probe perturbation. This perturbation can be characterized with induced dipole moments [18]. All design parameters are summarized in Table I. The simulated electric field distributions, both inside the cavity and inside the top substrate, are shown in Fig. 11(a) and (b), respectively. The efficient containment of the electric field and the perfect decoupling between the two feeding structures is observed. The cavity resonator using probe excitation was fabricated using LTCC technology, and its photograph is shown in Fig. 12.

The S-parameter data from both the simulations and the measurements are shown in Fig. 13. The measured insertion loss of 0.95 dB is a little larger than the simulated value 0.67 dB, but the measured bandwidth of 1.8% is narrower than the predicted value 3.74%. This difference might be due to a change in the external coupling caused by a misaligned probe position that can significantly affect the electromagnetic performance. No significant frequency shift in the operating frequencies of 59.8 GHz is observed. The simulated Q_u was found to be 355 compared to the theoretical Q_u of 362. The Q_{ext} was measured to be 49.8.

TABLE II
COMPARISON OF MEASURED RESULTS OF THREE DIFFERENT EXCITATION TECHNIQUES

	slot excitation with a shorting via	slot excitation with an open stub	probe excitation
Resonant Frequency (f_{res})	59.4 GHz	59.2 GHz	59.8 GHz
Insertion Loss (S21)	1.28 dB	0.84 dB	0.95 dB
Return Loss (S11)	18 dB	20.59 dB	22.3 dB
Bandwidth (BW)	1.18 %	1.5 %	1.8 %
Simulated Unloaded Q (Q_u)	360	367	355
Measured External Q (Q_{ext})	73.23	60.52	49.80

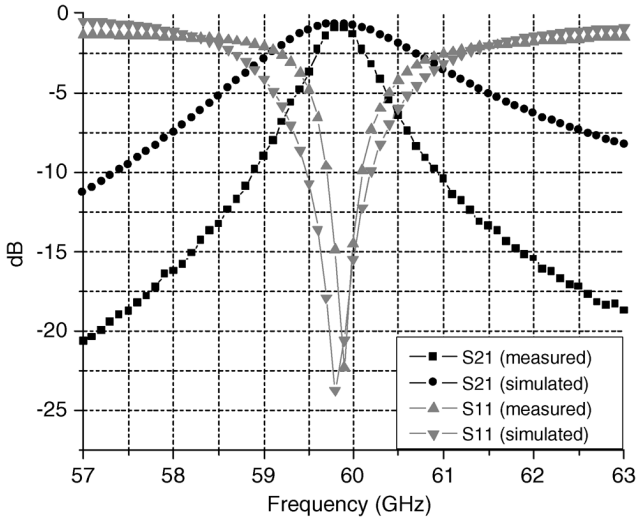

Fig. 13. Comparison between measured and simulated S-parameters (S11 and S21) of a cavity resonator using probe excitation.

D. Discussion

Table II summarizes the experimental results of the three cavity excitation techniques. Based on experimental results, the probe excitation exhibits the strongest coupling in terms of the lowest $Q_{\rm ext}$ measured from the strongly coupled resonators by using (6) and (7). In addition, the probe excitation is an attractive option for wideband applications due to its relatively wide bandwidth performance, but it requires a mature fabrication capability (accurate via stacking and alignment) to implement the probe structure.

The slot excitation with open stubs demonstrates the lowest insertion loss. An open stub contributes to fabrication simplicity with no need of drilling via holes to implement the feeding structures. Also, it avoids the loss and inductance effects generated by the via structure that could be serious in the mmW frequency range. However, the excitation techniques using a shorting via and vertically stacked vias (probe) take advantage of preventing electrical coupling between two microstrip feed-lines because of vias providing the necessary shielding, while reducing the substrate coupling effects generated from the extended open stub.

IV. CONCLUSION

In this paper, we presented for the first time a comparative study validated by measured data of three different excitation techniques for 3-D LTCC integrated cavity resonators. Three excitation techniques (slot excitation with a shorting via, slot excitation with a $\lambda_{\rm g}/4$ open stub, probe excitation) were comparatively evaluated in terms of S-parameters, bandwidth, external coupling $(Q_{\rm ext})$, $Q_{\rm u}$, and fabrication accuracy/simplicity based on electromagnetic simulations and experimental results. For mmW wideband applications, the probe excitation exhibited a relatively wide bandwidth nature ($\sim$1.8%) with the strongest external coupling based on the lowest $Q_{\rm ext}$. The slot excitation with open stub exceeded the other techniques in terms of the lowest insertion loss ($\sim$0.84 dB) over the 3 dB bandwidth around the center frequency of 59.2 GHz as well as fabrication simplicity. The shorting via exhibited excellent blockage of the electrical coupling between two microstrip feedlines along with a much simpler fabrication process than the probe excitation. The presented structures can be used in the development of 3-D multipole cavity band pass filters, and can be easily integrated within 3-D LTCC 60-GHz front-end modules.

ACKNOWLEDGMENT

The authors would like to thank the Asahi Glass Corporation for their technical support in fabricating the devices presented in this paper

REFERENCES

[1] M. F. Davis, A. Sutono, S.-Y. Yoon, S. Mandal, N. Bushyager, C.-H. Lee, K. Lim, S. Pinel, M. Maeng, A. Obatoyinbo, S. Chakraborty, J. Laskar, E. M. Tentrzeris, T. Nonaka, and R. R. Tummala, "Integrated RF architectures in fully-organic SOP technology," *IEEE Trans. Adv. Packag.*, vol. 25, no. 2, pp. 136–142, May 2002.

[2] K. Lim, S. Pinel, M. F. Davis, A. Sutono, C.-H. Lee, D. Heo, A. Obatoynbo, J. Laskar, E. M. Tentzeris, and R. Tummala, "RF-system-on-package (SOP) for wireless communications," *IEEE Microw. Mag.*, vol. 3, no. 1, pp. 88–99, Mar. 2002.

[3] D. Deslandes and K. Wu, "Millimeter-wave substrate integrated waveguide filters," in *Proc. IEEE Can. Conf. Elect. Comput. Eng.*, Montreal, QC, Canada, May 2003, pp. 1917–1920.

[4] Y. Cassivi and K. Wu, "Low cost microwave oscillator using substrate integrated waveguide cavity," *IEEE Microw. Wireless Compon. Lett.*, vol. 13, no. 2, pp. 48–50, Feb. 2003.

[5] S. Germain, D. Deslandes, and K. Wu, "Development of substrate integrated waveguide power dividers," in *Proc. IEEE Canadian Conf. Elect. Comput. Eng.*, Montreal, QC, Canada, May 2003, pp. 1921–1924.

[6] Z. C. Hao, W. Hong, X. P. Chen, J. X. Chen, K. Wu, and T. J. Cui, "Multilayered substrate integrated waveguide (MSIW) elliptical filters," *IEEE Microw. Wireless Compon. Lett.*, vol. 15, no. 2, pp. 95–97, Feb. 2005.

[7] M. J. Hill, R. W. Ziolkowski, and J. Papapolymerou, "Simulated and measured results from a duroid-based planar MBG cavity resonator filter," *IEEE Microw. Wireless Compon. Lett.*, vol. 10, no. 12, pp. 528–530, Dec. 2000.

[8] A. El-Tager, J. Bray, and L. Roy, "High-Q LTCC resonators for millimeter wave applications," in *IEEE MTT-S Int. Microw. Symp. Dig*, Philadelphia, PA, Jun. 2003, pp. 2257–2260.

[9] X. Gong, W. J. Chappell, and L. P. B. Katehi, "Multifunctional substrates for high-frequency applications," *IEEE Microw. Wireless Compon. Lett.*, vol. 13, no. 10, pp. 428–430, Oct. 2003.

[10] C. H. Lee, A. Sutono, S. Han, K. Lim, S. Pinel, J. Laskar, and E. M. Tentzeris, "A compact LTCC-based Ku-band transmitter module," *IEEE Trans. Adv. Packag.*, vol. 25, no. 3, pp. 374–384, Aug. 2002.
[11] B. G. Choi, M. G. Stubbs, and C. S. Park, "A Ka-band narrow bandpass filter using LTCC technology," *IEEE Microw. Wireless Compon. Lett.*, vol. 13, no. 9, pp. 388–389, Sep. 2003.
[12] W.-Y. Leung, K.-K. M. Cheng, and K.-L. W. , "Multilayer LTCC bandpass filter design with enhanced stopband characteristics," *IEEE Microw. Wireless Compon. Lett.*, vol. 12, no. 7, pp. 240–242, Jul. 2002.
[13] D. M. Pozar, "Microstrip antenna aperture-coupled to a microstripline," *Electron Lett.*, vol. 21, no. 2, pp. 49–50, Jan. 1985.
[14] X. H. Yang and L. Shafai, "Characteristics of aperture coupled microstrip antennas with various radiating patches and coupling apertures," *IEEE Trans. Antennas Propag.*, vol. 43, no. 1, pp. 72–78, Jan. 1995.
[15] L. Harle and L. P. B. Katehi, "A silicon micromachined four-pole linear phase filter," *IEEE Trans. Microw. Theory Tech.*, vol. 52, no. 6, pp. 1598–1607, Jun. 2004.
[16] M. Ito, K. Maruhashi, K. Ikuina, T. Hashiguchi, S. Iwanaga, and K. Ohata, "60-GHz-band dielectric waveguide filters with cross-coupling for flip-chip modules," in *IEEE MTT-S Int. Microw. Symp. Dig*, Seattle, WA, Jun. 2002, pp. 1789–1792.
[17] P. Couffignal, J. Obregon, and H. Baudrand, "Equivalent circuit of a cavity coupled to a feeding line and its depedance on the electric or magnetic nature of output coupling structure," *Proc. Inst. Elect. Eng. H*, vol. 139, no. 3, pp. 221–226, Jun. 1992.
[18] R. E. Collin, *Foundations for Microwave Engineering*. New York: McGraw-Hill, 1992.
[19] D. M. Pozar, *Microwave Engineering*, 2nd ed. New York: Wiley, 1998.
[20] D. M. Pozar and D. H. Schaubert, *Microstrip Antennas*. New York: IEEE Press, 1995.
[21] J.-S. Hong and M. J. Lancaster, *Microstrip Filters for RF/Microwave Applications*. New York: Wiley, 2001.

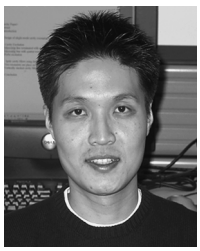

Jong-Hoon Lee (S'98) received the B.S. degree in electrical engineering from the Pennsylvania State University, University Park, in 2001 and the M.S. degree from Georgia Institute of Technology (Georgia Tech), Atlanta, in 2004, where he is currently working toward Ph.D. degree in electrical and computer engineering.

He is a member of the Georgia Tech ATHENA Research Group, NSF Packaging Research Center, and the Georgia Electronic Design Center, Atlanta. He has authored or coauthored more than 30 papers in refereed journals and conference proceedings and one book chapter. His research interests are packaging technology for microwave/millimeter-wave systems, multigigabit radios, passive/active circuits for RF/wireless systems, and DSP-based predictors to improve the computational efficiency of the simulation. He is currently researching the development of 3-D system-on-package (SOP) modules for millimeter-wave multigigabit wireless systems, and phased-array MIMO transceiver architectures for millimeter-wave wireless systems.

Stéphane Pinel (M'06) was born in Toulouse, France, in 1974. He received the B.S degree from Paul Sabatier University, Toulouse, France in 1997, and the Ph.D degree (with the highest honors) in microelectronics and microsystems from the Laboratoire d'Analyse et d'Architecture des Systemes, Centre National de la Recherche Scientifique (CNRS), Toulouse, in 2000.

He has worked on a UltraThin Chip Stacking (UTCS) European Project for three years involving Alcatel Space and IMEC (Belgium). Since 2000, he has been working as a Research Faculty at the Georgia Electronic Design Center, Georgia Institute of Technology. He has authored and coauthored over 110 journals and proceeding papers, two book chapters, numerous invited talks, participated and organized numerous workshops at international conferences such IMS, and holds four patents/invention disclosures. His research interests include advanced 3-D integration and packaging technologies, RF and millimeter-wave embedded passives (filters, antenna arrays) design using organic (liquid crystal polymer) and ceramic materials (LTCC), RF-MEMS and micromachining techniques, system-on-package for RF and millimeter-waves front-end module, and SOI, CMOS, and SiGe RF and millimeter-waves circuit design. He is now leading research efforts for the development of multigigabits wireless radio.

Dr. Pinel was the recipient of the First Prize of the SEE 1998 Awards, the Second Prize of the IMAPS 1999 Awards, and the 2002 International Conference on Microwave and Millimeter-Wave Technology Best Paper Award (Beijing, China).

John Papapolymerou (S'90–M'95–SM'04) received the B.S.E.E. degree from the National Technical University of Athens, Athens, Greece, in 1993 and the M.S.E.E. and Ph.D. degrees from the University of Michigan, Ann Arbor, in 1994 and 1999, respectively.

From 1999 to 2001, he was a Faculty Member at the Department of Electrical and Computer Engineering, University of Arizona, Tucson, and during the summers of 2000 and 2003, he was a Visiting Professor at The University of Limoges, Limoges, France. In August 2001, he joined the School of Electrical and Computer Engineering, Georgia Institute of Technology, Atlanta, where he is currently an Assistant Professor. His research interests include the implementation of micromachining techniques and MEMS devices in microwave, millimeter-wave and terahertz circuits and the development of both passive and active planar circuits on semiconductor (Si/SiGe, GaAs) and organic substrates (LCP, LTCC) for high-frequency applications. He has authored or coauthored over 80 publications in peer reviewed journals and conferences. He currently serves as the secretary for Commission D of the U.S. National Committee of URSI.

Dr. Papapolymerou received the 2004 Army Research Office (ARO) Young Investigator Award, the 2002 National Science Foundation (NSF) CAREER award, the Best Paper Award at the Third IEEE International Conference on Microwave and Millimeter-Wave Technology (ICMMT2002), Beijing, China, and the 1997 Outstanding Graduate Student Instructional Assistant Award presented by the American Society for Engineering Education (ASEE), The University of Michigan Chapter. His student also received the Best Student Paper Award at the 2004 IEEE Topical Meeting on Silicon Monolithic Integrated Circuits in RF Systems, Atlanta.

Joy Laskar (S'84–M'85–SM'02–F'05) received the B.S. degree in computer engineering with math/physics minors (highest honors) from Clemson University, Clemson, SC, in 1985 and the M.S. and the Ph.D. degrees in electrical engineering from the University of Illinois at Urbana-Champaign in 1989 and 1991, respectively.

Prior to joining the Georgia Institute of Technology (Georgia Tech) in 1995, he has held faculty positions at the University of Illinois at Urbana-Champaign and the University of Hawaii. At Georgia Tech, he holds the Joseph M. Pettit Professorship of Electronics, is the Director of Georgia's Electronic Design Center, and heads a research group of 25 members with a focus on integration of high-frequency mixed-signal electronics for next-generation wireless and wired systems. He has authored or coauthored more than 200 papers, several book chapters (including three textbooks in development), numerous invited talks, and has more than 20 patents pending. Most recently, his work has resulted in the formation of two companies. In 1998, he cofounded an advanced WLAN IC Company, RF Solutions, which is now part of Anadigics. In 2001, he cofounded a next-generation analog CMOS IC company, Quellan, which is developing collaborative signal processing solutions for the enterprise, video, storage, and wireless markets.

Dr. Laskar is a 1995 recipient of the Army Research Office's Young Investigator Award, a 1996 recipient of the National Science Foundation's CAREER Award, the 1997 NSF Packaging Research Center Faculty of the Year, the 1999 corecipient of the IEEE Rappaport Award (Best IEEE Electron Devices Society Journal Paper), the faculty advisor for the 2000 IEEE Microwave Theory and Techniques Society (MTTS) IMS Best Student Paper Award, 2001 Georgia Tech Faculty Graduate Student Mentor of the year, recipient of a 2002 IBM Faculty Award, the 2003 Clemson University College of Engineering Outstanding Young Alumni Award, and the 2003 recipient of the Outstanding Young Engineer of the IEEE MTTS. For the 2004–2006 term, he has been appointed an IEEE Distinguished Microwave Lecturer for his seminar entitled "Recent Advances in High Performance Communication Modules and Circuits."

Manos M. Tentzeris (S'89–M'92–SM'03) received the Diploma degree (magna cum laude) in electrical and computer engineering from the National Technical University of Athens, Athens, Greece, and the M.S. and Ph.D. degrees in electrical engineering and computer science from the University of Michigan, Ann Arbor.

He is currently an Associate Professor with School of Electrical and Computer Engineering, Georgia Institute of Technology (Georgia Tech), Atlanta. He has published more than 250 papers in refereed journals and conference proceedings, one book and eight book chapters, and he is in the process of writing two books. He has helped develop academic programs in highly integrated/multilayer packaging for RF and wireless applications using ceramic and organic flexible materials, paper-based RFIDs and sensors, microwave MEMs, SOP-integrated (UWB, mutliband, conformal) antennas, and adaptive numerical electromagnetics (FDTD, multiresolution algorithms) and heads the ATHENA Research Group (15 researchers). He is the Georgia Electronic Design Center Associate Director for RFID/Sensors research, and he has been the Georgia Tech NSF-Packaging Research Center Associate Director for RF Research and the RF Alliance Leader from 2003 to 2006. He is also the leader of the RFID Research Group of the Georgia Electronic Design Center (GEDC) of the State of Georgia. He was a Visiting Professor with the Technical University of Munich, Germany, for the summer of 2002, where he introduced a course in the area of high-frequency packaging. He has given more than 50 invited talks in the same area to various universities and companies in Europe, Asia, and America.

Dr. Tentzeris was the recipient of the 2006 IEEE MTT Outstanding Young Engineer Award, the 2004 IEEE TRANSACTIONS ON ADVANCED PACKAGING Commendable Paper Award, the 2003 NASA Godfrey "Art" Anzic Collaborative Distinguished Publication Award, the 2003 IBC International Educator of the Year Award, the 2003 IEEE CPMT Outstanding Young Engineer Award, the 2002 International Conference on Microwave and Millimeter-Wave Technology Best Paper Award (Beijing, China), the 2002 Georgia Tech-ECE Outstanding Junior Faculty Award, the 2001 ACES Conference Best Paper Award, the 2000 NSF CAREER Award, and the 1997 Best Paper Award of the International Hybrid Microelectronics and Packaging Society. He was also the 1999 Technical Program Co-Chair of the 54th ARFTG Conference, Atlanta, and the Chair of the 2005 IEEE CEM-TD Workshop. He is the Vice-Chair of the RF Technical Committee (TC16) of the IEEE CPMT Society. He has organized various sessions and workshops on RF/wireless packaging and integration, RFIDs, numerical techniques/wavelets, in IEEE ECTC, IMS, VTC, and APS symposia in all of which he is a member of the Technical Program Committee in the area of "Components and RF." He is the TPC Chair for IEEE IMS 2008 Symposium. He is the Associate Editor of IEEE TRANSACTIONS ON ADVANCED PACKAGING. He is a member of URSI-Commission D, an Associate Member of EuMA, and a member of the Technical Chamber of Greece.